International Journal of Heat and Mass Transfer 52 (2009) 2140–2144

Contents lists available at ScienceDirect

International Journal of Heat and Mass Transfer

journal homepage: www.elsevier.com/locate/ijhmt

Technical Note

Study of the sensitivity of a thermal flow sensor

Tae Hoon Kim, Dong-Kwon Kim, Sung Jin Kim *

School of Mechanical, Aerospace & Systems Engineering, Korea Advanced Institute of Science and Technology, Daejeon 305-701, South Korea

ARTICLE INFO

Article history:
Received 23 April 2008
Received in revised form 8 October 2008
Available online 21 November 2008

ABSTRACT

The sensitivity of a thermal flow sensor is investigated in this study. A simple numerical model for analyzing heat transfer phenomena in the thermal flow sensor is presented. In order to validate the proposed model, experimental investigations are performed. Based on the results from the validated model, a correlation that predicts the sensitivity of the thermal flow sensor is presented. From the correlation, the manner in which the heat loss, the positions of the temperature sensors, the input power, and the heater length affect the sensitivity of the thermal flow sensor is investigated.

1. Introduction

The measurement and control of flow is critical in many engineering applications, including semiconductor manufacturing processes, chemical processes, and MEMS devices. The most widely used flow sensor is a thermal flow sensor, which has the advantage of a small size, a short response time, and low power consumption [1]. The thermal flow sensor typically consists of upstream and downstream temperature sensors and a heater located between the two temperature sensors as shown in Fig. 1(a). The mass flow rate is sensed via the temperature difference caused by the heat transfer interaction between a heated sensor and a fluid stream, as shown in Fig. 1(a) [2,3].

As shown in Fig. 1(b), the sensitivity of a thermal flow sensor is defined as the derivative of the temperature difference with respect to the mass flow rate at a zero flow rate. In other words, the sensitivity is given as the following equation:

$$S = \left.\frac{\partial(T_t(x = L_s) - T_t(x = -L_s))}{\partial \dot{m}}\right|_{\dot{m}=0} \tag{1}$$

As the sensitivity decreases, the ratio of the temperature difference to the mass flow rate decreases. If this temperature difference becomes smaller than the resolution of the temperature sensors, the thermal flow sensor cannot be used to measure the mass flow rate. Therefore, sensitivity is a critical parameter in the design of a thermal flow sensor. A number of researchers have studied the sensitivity of thermal flow sensors. Lammerink et al. [4] presented parameters that affect the sensitivity of a thermal flow sensor using simple 1-D modeling. Sabate et al. [5], Roh et al. [6], and Kim and Kim [7] experimentally showed the effects of the positions of temperature sensors and/or the heater power on the sensitivity of the thermal flow sensor. However, their results were limited to a qualitative evaluation. There is no reliable data or correlation by which it is possible to predict the sensitivity in the design of thermal flow sensors quantitatively.

The present study contends with the sensitivity of a thermal flow sensor. In it, a simple numerical model of a thermal flow sensor is presented. In order to validate the proposed model, experimental investigations are performed. Based on the results from the validated model, a correlation that predicts the sensitivity of a thermal flow sensor is presented. From the correlation, the manner in which the heat loss, the positions of temperature sensors, the input power, and the heater length affect the sensitivity of the thermal flow sensor is investigated.

2. Simple numerical model

To analyze heat transfer phenomena in a thermal flow sensor, the physical domain of the thermal flow sensor is divided into two regions: a sensor tube region and an inner fluid region. The energy balance for each region is represented by

$$k_t A_t \frac{d^2 T_t}{dx^2} + h_i P(T_f - T_t) - \frac{1}{R_r}(T_t - T_{amb}) + q' = 0 \tag{2}$$

$$k_f A_f \frac{d^2 T_f}{dx^2} - \dot{m} C_f \frac{dT_f}{dx} + h_i P(T_t - T_f) = 0 \tag{3}$$

where T_s, T_f, A, h_i, P, R_r, and q' are the tube temperature, inner fluid temperature, cross-sectional area, interstitial heat transfer coefficient, wetted perimeter of the tube, thermal resistance per unit length for radial heat loss, and heat flux per unit length supplied from the heater, respectively [8]. The first term on the left side of Eq. (2) is the axial conduction term, and the second term represents the thermal interaction between the sensor tube and the fluid. The third term denotes the radial heat loss from the outer wall of the tube to the surrounding area. Similarly, Eq. (3) consists of a conduction term in the axial direction, the enthalpy change term of the

* Corresponding author. Tel.: +82 42 350 3043; fax: +82 42 350 8207.
E-mail address: sungjinkim@kaist.ac.kr (S.J. Kim).

0017-9310/$ - see front matter © 2008 Elsevier Ltd. All rights reserved.
doi:10.1016/j.ijheatmasstransfer.2008.10.006

Nomenclature

A	cross-sectional area, m^2
C	heat capacity, J/kg K
h_i	interstitial heat transfer coefficient, W/m^2 K
k	thermal conductivity, W/m K
L	distance from the center of the thermal flow sensor to the end of the channel, m
L_h	distance from the center of the thermal flow sensor to the end of the heater, m
L_s	distance from the center of the thermal flow sensor to the temperature sensor, m
$\dot{m}$	mass flow rate of the fluid, kg/s
P	wetted perimeter of the tube, m
q'	heat flux per unit length supplied from the heater, W/m
R_r	thermal resistance per unit length for radial heat loss, m K/W
S	sensitivity of the thermal flow sensor, °C/(kg/s)
T	temperature, °C
x	axial coordinate

Subscripts

amb	ambient
f	fluid
t	tube

fluid, and the thermal interaction term. Boundary conditions are given as follows:

$$T_t(x=-L)=T_f(x=-L)=T_{amb} \tag{4}$$

$$T_t'(x\to\infty)=T_f'(x\to\infty)=0 \tag{5}$$

Governing equations are solved using the control-volume-based finite difference method. A power law scheme is used for discretization of the conduction and convection terms. Discretization equations are calculated using the ADI method. All numerical data in this paper were obtained using the numerical model presented in this section.

3. Experimental validation

An experimental investigation was performed to validate the proposed numerical model. A thermal flow sensor was manufactured through simple microfabrication processes. Thin-film thermocouples and a heater were fabricated on a quartz wafer in sputtering processes. The heater consisted of nichrome and the thin-film thermocouples have compositions that are identical to those of standard K-type thermocouples. A channel consisted of PDMS (polydimethylsiloxane). The quartz wafer and the PDMS channel were bonded by using air plasma. Fig. 2 shows the thermal flow sensor. Detailed fabrication processes are explained in Ref. [7]. As flow sensors are generally calibrated with nitrogen gas, nitrogen gas was used as the operating fluid in this experiment. The purity

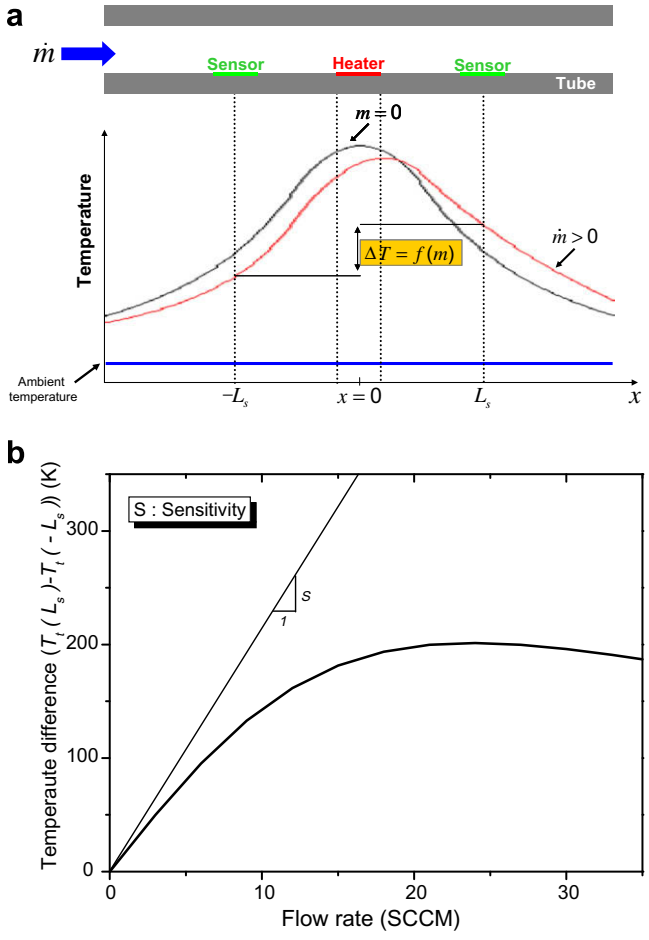

Fig. 1. Operating principle of the thermal flow sensor. (a) Schematic layout of the thermal flow sensor. (b) Typical output of the thermal flow sensor (not in scale).

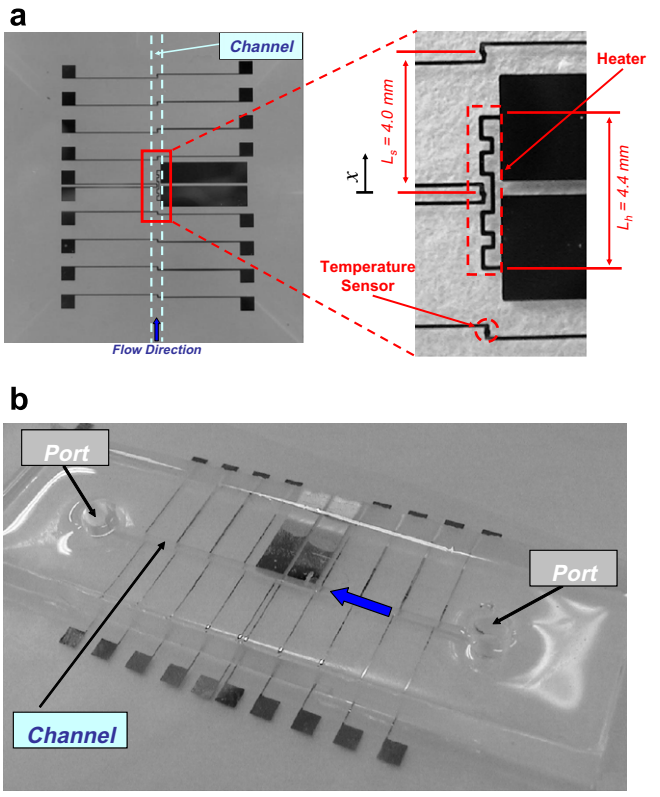

Fig. 2. Thermal flow sensor [7]. (a) Thin-film thermocouples and a heater deposited onto a quartz wafer. (b) The thermal flow sensor integrated with a PDMS channel.

of the nitrogen gas was 99.9993%. As shown, nitrogen gas passes through the PDMS channel. A calibrated standard mass flow meter was used to control the mass flow rate of the nitrogen gas in the experiment. The range of the mass flow meter was from 0 to 100 SCCM (standard cubic centimeter per minute). The heater was powered by a DC power supply with power of 0.8 W. The length of the heater was 4.4 mm as shown in Fig. 2. There were nine temperature sensors in a thermal flow sensor that measure the temperature distributions on the bottom surface of the channel. The distance between two adjacent temperature sensors was 4 mm, as shown in Fig. 2. The temperature signals from the thermal flow sensor can be measured directly using a data acquisition unit. When obtaining the experimental results, experiments were conducted five times.

4. Results and discussion

Fig. 3 shows the temperature distributions along the PDMS channel. As can be seen in the figure, the results from the simple numerical model are in fair agreement with the experimental results within a relative error of 10%. Therefore, the presented model is suitable for predicting the sensitivity of a thermal flow sensor. From Fig. 3, the heat transfer phenomena in the thermal flow sensor can be explained. As shown in Fig. 3(a), the temperature distribution is symmetric under a zero flow rate. When nitrogen gas flows through the PDMS channel, the surface temperature of the thermal flow sensor in the upstream section decreases while that in the downstream section increases due to convection [2]. The temperature of the thermal flow sensor reaches its equilibrium distribution when a balance exists among heat generation, flow convection, axial conduction, and heat loss. This distribution becomes asymmetric, as shown in Fig. 3(b) and (c). Moreover, a higher mass flow rate implies a lower the surface temperature at the upstream section of the channel and a higher surface temperature at the downstream section of the channel. These phenomena are identical to the heat transfer phenomena occurring in the circular sensor tube of the MFC (mass flow controller) studied by Kim and Jang [2]. Fig. 4 shows that the position of temperature sensors affects the sensitivity of the thermal flow sensor. As shown in Fig. 4, the temperature difference measured using the sensors located near the heater is larger compared to that obtained using sensors located further away from the heater for a fixed mass flow rate. This implies that the sensitivity decreases as the distance between the temperature sensors increases.

Finally, based on the numerical results, a correlation that predicts the sensitivity is obtained according to Eq. (1). The correlation is given as

$$\frac{S(k_tA_t)^2}{q'L^3C_f} = \exp\left[D_1 + D_2\left[\frac{L^2}{k_tA_tR_r}\right]^{D_3}\right] \tag{6}$$

where

$$D_1 = \left[-4.62 + \left\{2.04 + 15.8\left(\frac{L_h}{L_s}\right)\right\}\left(\frac{L_s}{L}\right) - 1.2\left(\frac{L_s}{L}\right)^2\right]$$

$$D_2 = \left[-2.66 + 7.54\left(\frac{L_s}{L}\right) - 15.08\left(\frac{L_s}{L}\right)^2 + 9.59\left(\frac{L_s}{L}\right)^3\right]$$

$$D_3 = \left[0.14 + 0.72\left(\frac{L_s}{L}\right) - 0.52\left(\frac{L_s}{L}\right)^2\right]$$

In Eq. (6), $S(k_tA_t)^2/q'L^3C_f$ is the dimensionless sensitivity and $L^2/k_tA_tR_r$ is the dimensionless radial heat loss. The correlation based on the numerical results can be applicable for

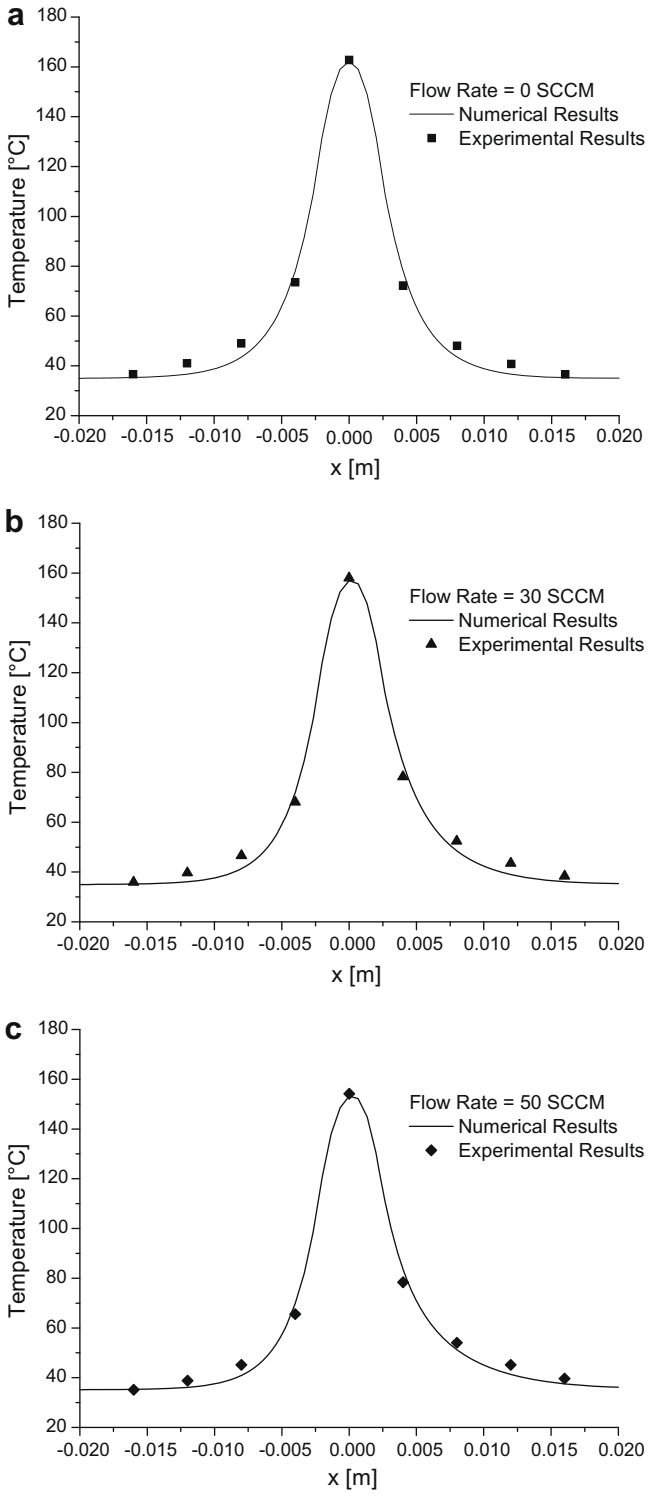

Fig. 3. Temperature distributions (input power = 0.8 W). (a) 0 SCCM. (b) 30 SCCM. (c) 50 SCCM.

$$0.1 < \frac{L^2}{k_tA_tR_r} < 1000, \quad 0.2 < \frac{L_s}{L} < 0.6, \quad 0.1 < \frac{L_h}{L_s} < 0.6 \tag{7}$$

Fig. 5 shows the sensitivity obtained both from the numerical results and from the correlation. The correlation predicts the numerical results within a relative error of 10%. By using the proposed correlation, the effects of the positions of the temperature sensors on the sensitivity can be investigated. As shown in Fig. 5,

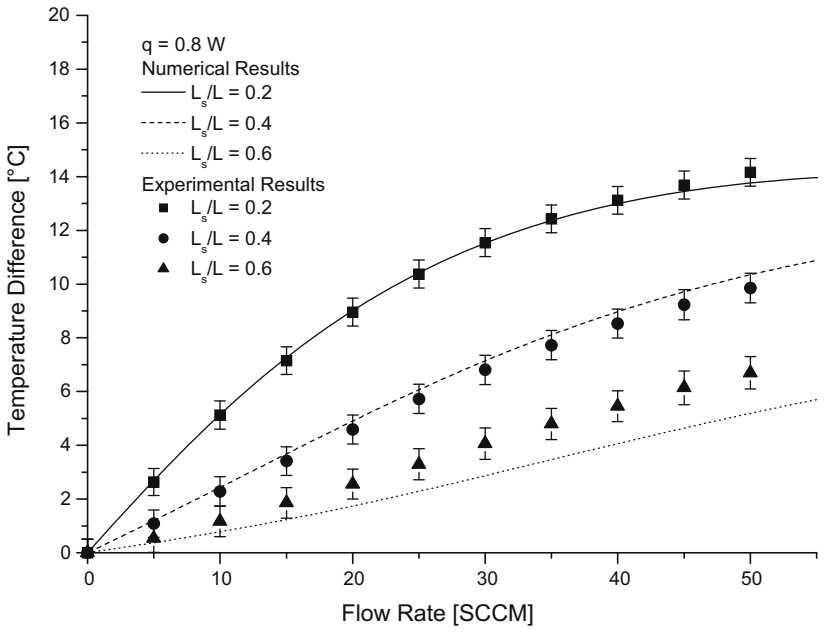

Fig. 4. Relationship between the temperature difference and the flow rate.

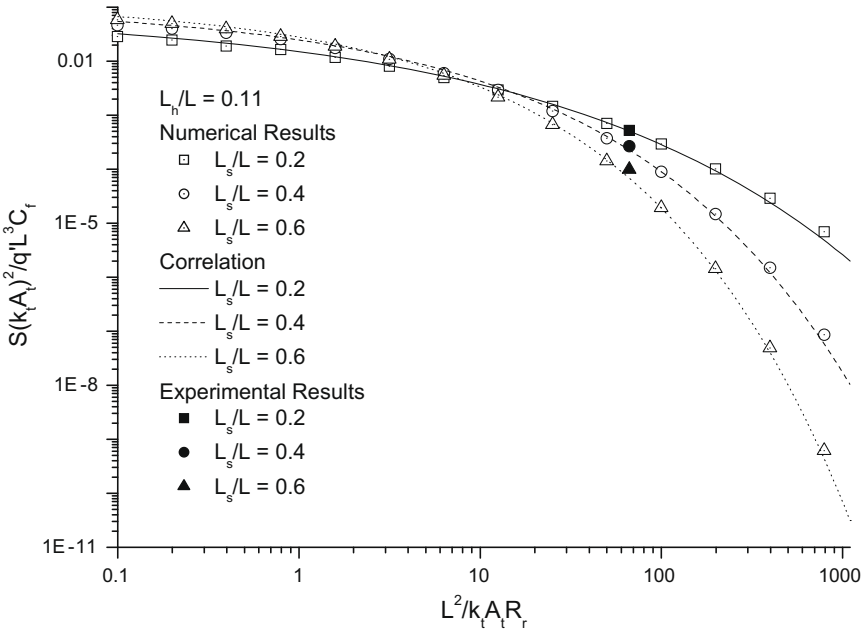

Fig. 5. Comparison between the sensitivity values from the correlation, the numerical results, and the experimental results.

heat loss is closely related to sensitivity. The sensitivity increases as the heat loss decreases. In addition, when $L^2/k_tA_tR_r < 10$, the sensitivity increases as L_s/L increases. In contrast, when $L^2/k_tA_tR_r > 10$, the sensitivity decreases as L_s/L increases. As the experimental condition in this paper is under $L^2/k_tA_tR_r > 10$, the experimental results show that the sensitivity decreases as L_s/L increases.

Fig. 6 shows the sensitivity for various L_h/L_s and L_s/L value. As shown in Fig. 6(a), when $L^2/k_tA_tR_r < 10$ the sensitivity increases as L_h/L_s increases regardless of the value of L_s/L. However, as shown in Fig. 6(b), when $L^2/k_tA_tR_r > 10$ the tendency of the sensitivity is different from that of the sensitivity under the condition of $L^2/k_tA_tR_r < 10$. Although the sensitivity increases as L_h/L_s increases, when $L_h/L_s < 0.35$, the sensitivity decreases as L_s/L increases. On the other hand, when $L_h/L_s > 0.35$, the sensitivity increases as L_s/L increases.

5. Conclusion

In this study, the sensitivity of a thermal flow sensor is studied. A simple numerical model for analyzing heat transfer phenomena in a thermal flow sensor is presented. Additionally, the proposed model is validated by experimental data. Based on the verified numerical model, a correlation that predicts the sensitivity of a thermal flow sensor is obtained. From the correlation, it is shown that the heat loss, the positions of temperature sensors, the input power, and the heater length affect the sensitivity of a thermal flow sensor.

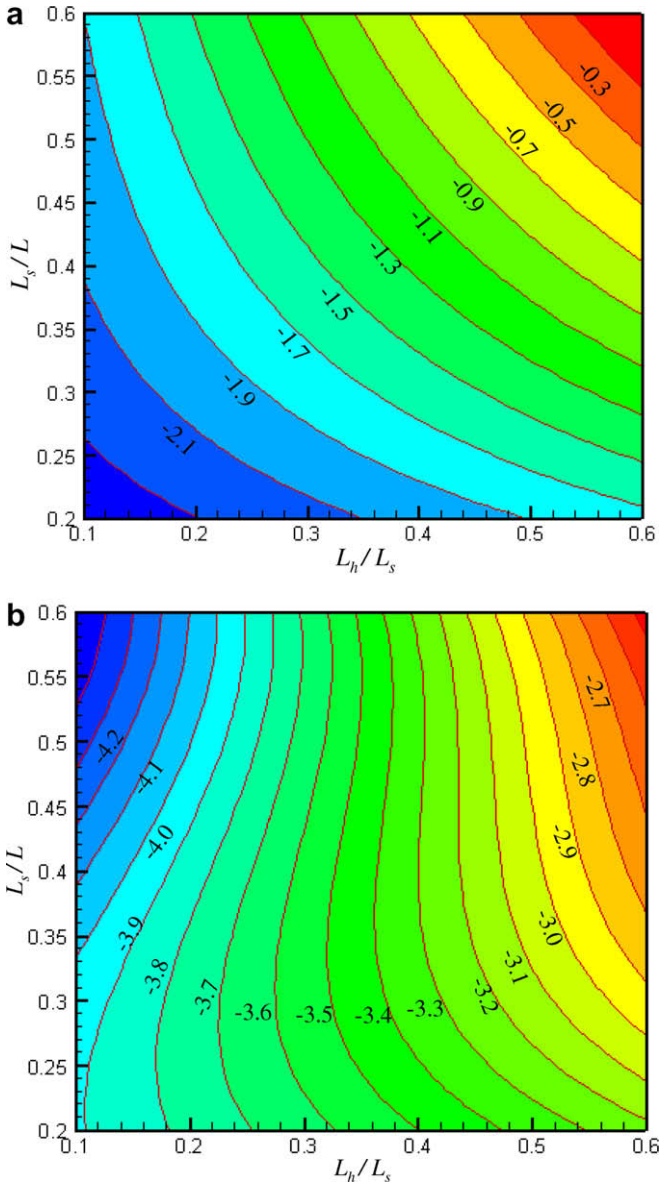

Fig. 6. The sensitivity $\left(\log_{10}\left[S(k_tA_t)^2/q'L^3C_f\right]\right)$ for various L_h/L_s and L_s/L. (a) $L^2/k_tA_tR_r < 10$. (b) $L^2/k_tA_tR_r > 10$.

Acknowledgement

This work was supported by the Korea Science and Engineering Foundation (KOSEF) through the National Research Laboratory Program funded by the Ministry of Science and Technology (No. M1060000022406J000022410).

References

[1] N.T. Nguyen, Micromachined flow sensors – review, Flow Meas. Instrum. 8 (1997) 7–16.
[2] S.J. Kim, S.P. Jang, Experimental and numerical analysis of heat transfer phenomena in a sensor tube of a mass flow controller, Int. J. Heat Mass Transfer 44 (2001) 1711–1724.
[3] I.Y. Han, D.-K. Kim, S.J. Kim, Study on the transient characteristics of the sensor tube of a thermal mass flow meter, Int. J. Heat Mass Transfer 48 (2005) 2583–2592.
[4] T.S.J. Lammerink, N.R. Tas, M. Elwenspoek, J.H.J. Fluitman, Micro-liquid flow sensor, Sens. Actuators A 37–38 (1993) 45–50.
[5] N. Sabate, J. Santander, L. Fonseca, I. Gracia, C. Cane, Multi-range silicon micromachined flow sensor, Sens. Actuators A 110 (2004) 282–288.
[6] S.-C. Roh, Y.-M. Choi, S.-Y. Kim, Sensitivity enhancement of a silicon micromachined thermal flow sensor, Sens. Actuators A 128 (2006) 1–6.
[7] T.H. Kim, S.J. Kim, Development of a micro-thermal flow sensor with thin-film thermocouples, J. Micromech. Microeng. 16 (2006) 2502–2508.
[8] D.-K. Kim, I.Y. Han, S.J. Kim, Study on the steady-state characteristics of the sensor tube of a thermal mass flow meter, Int. J. Heat Mass Transfer 50 (2007) 1206–1211.